Molecular Plant Pathology

MOLECULAR PLANT PATHOLOGY (2015) **16**(4), 388–399 DOI: 10.1111/mpp.12188

Symptoms induced by transgenic expression of p23 from *Citrus tristeza virus* in phloem-associated cells of Mexican lime mimic virus infection without the aberrations accompanying constitutive expression

NURIA SOLER[1], CARMEN FAGOAGA[1], CARMELO LÓPEZ[2], PEDRO MORENO[1], LUIS NAVARRO[1], RICARDO FLORES[2] AND LEANDRO PEÑA[1,3,*]

[1]*Centro de Protección Vegetal y Biotecnología, Instituto Valenciano de Investigaciones Agrarias (IVIA), Apdo. Oficial, Moncada, Valencia 46113, Spain*
[2]*Instituto de Biología Molecular y Celular de Plantas (UPV-CSIC), Universidad Politécnica de Valencia, Avenida de los Naranjos, Valencia 46022, Spain*
[3]*Fundo de Defesa da Citricultura (Fundecitrus), Av. Dr. Adhemar de Barros Pereira, 201 14807-040 Vila Melhado, Araraquara, Sao Paulo, Brazil*

SUMMARY

Citrus tristeza virus (CTV) is phloem restricted in natural citrus hosts. The 23-kDa protein (p23) encoded by the virus is an RNA silencing suppressor and a pathogenicity determinant. The expression of p23, or its N-terminal 157-amino-acid fragment comprising the zinc finger and flanking basic motifs, driven by the constitutive 35S promoter of cauliflower mosaic virus, induces CTV-like symptoms and other aberrations in transgenic citrus. To better define the role of p23 in CTV pathogenesis, we compared the phenotypes of Mexican lime transformed with p23-derived transgenes from the severe T36 and mild T317 CTV isolates under the control of the phloem-specific promoter from *Commelina yellow mottle virus* (CoYMV) or the 35S promoter. Expression of the constructs restricted to the phloem induced a phenotype resembling CTV-specific symptoms (vein clearing and necrosis, and stem pitting), but not the non-specific aberrations (such as mature leaf epinasty and yellow pinpoints, growth cessation and apical necrosis) observed when p23 was ectopically expressed. Furthermore, vein necrosis and stem pitting in Mexican lime appeared to be specifically associated with p23 from T36. Phloem-specific accumulation of the p23Δ158–209(T36) fragment was sufficient to induce the same anomalies, indicating that the region comprising the N-terminal 157 amino acids of p23 is responsible (at least in part) for the vein clearing, stem pitting and, possibly, vein corking in this host.

Keywords: citrus, *Commelina yellow mottle virus* promoter, CTV, pathogenicity determinant, phloem-specific expression, RNA silencing suppressor, tristeza.

INTRODUCTION

Citrus tristeza virus (CTV) is the causal agent of devastating epidemics that have changed the course of the citrus industry, provoking the worldwide loss of almost 100 million trees of sweet orange [*Citrus sinensis* (L.) Osb.], mandarin (*C. reticulata* Blanco), grapefruit (*C. paradisi* Macf.) and lime [*C. aurantifolia* (Christ.) Swing.] propagated on sour orange (*C. aurantium* L.) (Moreno *et al*., 2008). CTV is a member of the genus *Closterovirus*, family *Closteroviridae*, and only infects naturally phloem-associated tissues of species of the genera *Citrus* and *Fortunella* within the family Rutaceae, subfamily Aurantoideae. The virus is readily transmitted with infected buds and spread locally by several aphid species in a semi-persistent mode (Bar-Joseph *et al*., 1989).

CTV has a plus-strand, single-stranded genomic RNA (gRNA) of approximately 19.3 kb organized in 12 open reading frames (ORFs), potentially encoding at least 17 protein products, delimited by 5' and 3' untranslated regions (UTRs) (Karasev *et al*., 1995). The two 5'-proximal ORFs encode components of the replicase complex (Karasev *et al*., 1995) and are translated directly from the gRNA (Hilf *et al*., 1995). The 10 ORFs located in the 3' moiety of the gRNA are expressed through a set of 3' co-terminal subgenomic mRNAs (Hilf *et al*., 1995) encoding proteins p33, p6, p65, p61, p27, p25, p18, p13, p20 and p23 (Karasev *et al*., 1995; Pappu *et al*., 1994). The small hydrophobic p6 has been proposed to act as a transmembrane anchor, and p25 and p27 are the major and minor coat proteins, respectively. About 97% of the gRNA is encapsidated by p25 and the 5'-terminal approximately 630 nucleotides by p27 (Febres *et al*., 1996; Satyanarayana *et al*., 2004). These two proteins, together with p65 and p61, are required for virus assembly (Satyanarayana *et al*., 2000). Although p33, p13 and p18 are dispensable for the systemic infection of some citrus hosts, but required for others (Tatineni *et al*., 2008, 2011), p20, a protein accumulating in amorphous inclusion bodies of CTV-infected cells (Gowda *et al*., 2000), and p23 are indispensable for the invasion of all hosts (Tatineni *et al*., 2008). In addition, p33 is needed for superinfection exclusion (Folimonova, 2012).

Unique to CTV is p23, with no homologues found in other closteroviruses (Dolja *et al*., 2006). It is expressed in the early stages of cell infection (Navas-Castillo *et al*., 1997) and

*Correspondence: Email: lpenya@fundecitrus.com.br

accumulates in infected plants at moderate levels relative to other viral proteins (Pappu *et al*., 1997). Dolja *et al*. (1994) showed the presence of a cluster of positively charged amino acids in p23, and López *et al*. (1998) further defined this conserved region which has a core with three cysteines and one histidine forming a putative zinc finger domain. The presence of this domain suggests a regulatory function for p23, a view supported by the finding that p23 binds RNA *in vitro* in a sequence non-specific manner, and that mutations affecting the cysteine and histidine residues increase the dissociation constant of the p23–RNA complex (López *et al*., 2000). Moreover, p23 is involved in the regulation of the balance of plus and minus viral strands during replication, with the zinc finger domain and an adjacent basic region being indispensable for asymmetrical accumulation of the plus strand (Satyanarayana *et al*., 2002). Together with p20 and p25, p23 acts as an RNA silencing suppressor (RSS) in *Nicotiana tabacum* and *N. benthamiana*, with p25 acting intercellularly, p23 intracellularly and p20 at both levels (Lu *et al*., 2004). In addition, p23 is a viral pathogenicity determinant when expressed ectopically in citrus (see below). Moreover, the seedling yellows syndrome, induced by some CTV strains in sour orange and grapefruit, has been mapped at the p23 3' UTR region (Albiach-Martí *et al*., 2010).

The gRNA region coding for p23 is a hotspot for RNA silencing because small RNAs (sRNAs) from this region accumulate to high levels in CTV-infected Mexican lime and sweet orange (Ruiz-Ruiz *et al*., 2011). Ectopic expression of p23 enhances systemic infection and virus accumulation in transgenic sour orange and facilitates CTV escape from the phloem of transgenic sweet and sour orange. Therefore, constraints to CTV movement in some citrus hosts, particularly in sour orange, may, at least in part, result from RNA silencing (Fagoaga *et al*., 2011). Moreover, recent data have indicated that p23 accumulates preferentially in the nucleolus and Cajal bodies, as well as in plasmodesmata, being some basic motifs and the zinc-finger domain essential for nucleolar localization (Ruiz-Ruiz *et al*., 2013). The same motifs/domain are sufficient for the induction of necrosis in *N. benthamiana* when p23 is expressed from *Potato virus X* and for inciting CTV-like aberrations in transgenic Mexican lime plants, thus linking the pathogenicity of p23 to its nucleolar localization. In contrast, most p23 regions are needed for RSS activity in *N. benthamiana* (Ruiz-Ruiz *et al*., 2013).

The use of transgenic plants has been instrumental in the identification of viral RSS and pathogenicity determinants, although most of this work has been restricted to *Nicotiana* spp. and *Arabidopsis thaliana* (Díaz-Pendón and Ding, 2008). However, transgenic expression of RSS in non-natural hosts does not necessarily reflect the effects of viral infection, because, in their natural context, these proteins are often expressed only in infected cells and tissues, unlike the constitutively expressed transgenes (Csorba *et al*., 2009; Díaz-Pendón and Ding, 2008). Alternatively, mutant viruses expressing dysfunctional proteins have been used to assess their role as pathogenicity determinants (Hsieh *et al*., 2009; Yambao *et al*., 2008; Ziebell and Carr, 2009). Unfortunately, this approach can neither be extended to p23, because it is essential for CTV replication (Satyanarayana *et al*., 1999), nor be replaced by a homologue from a related virus, because p23 is unique among closteroviruses. Symptoms induced by certain CTV strains in citrus, such as vein clearing and stem pitting, are specific to this pathosystem and are recapitulated by some of the aberrations associated with the constitutive expression of p23 in Mexican lime. However, other non-specific symptoms accompanying the constitutive expression of p23, such as mature leaf epinasty and yellow pinpoints, growth cessation and apical necrosis (Fagoaga *et al*., 2005; Ghorbel *et al*., 2001), are rarely seen in non-transgenic CTV-infected Mexican lime and other citrus species. These latter aberrations most probably result from the ectopic expression of p23 in cells other than those associated with the phloem, the only tissue infected by CTV.

To better define the role of p23 in CTV pathogenesis, we restricted the transgenic expression of p23 to phloem-associated cells of Mexican lime. For this purpose, constructions carrying different versions of p23, or fragments thereof, were placed under the control of the phloem-specific promoter from *Commelina yellow mottle virus* (CoYMV) (Medberry *et al*., 1992). We show here that: (i) aberrations associated with phloem-specific expression and the accumulation of p23 are essentially identical to symptoms caused by CTV infection in Mexican lime; (ii) some of these CTV-like symptoms induced by p23 from the severe strain T36 were not observed when using p23 from the mild strain T317, thus mimicking the effects of natural infections by both CTV strains; and (iii) similar restricted expression of the fragment comprising the zinc finger and flanking basic motifs of p23 is sufficient to induce the CTV-like aberrations, confirming that the N-terminal region of 157 amino acids determines, at least in part, CTV pathogenesis in Mexican lime.

RESULTS AND DISCUSSION

Vein clearing in Mexican lime transformed with CoYMV-*p23* constructs resembles that induced by CTV in non-transformed plants and correlates in intensity with p23 accumulation

On the basis of the transgene integrity of *p23* and locus/loci patterns, as determined by enzyme restriction and Southern blot hybridization, at least 10 independent Mexican lime lines were generated for each of the three constructs CoYMV-*p23*(T36), CoYMV-*p23Δ158–209*(T36) and CoYMV-*p23*(T317), as well as for the empty vector (EV) (Fig. 1a). The selected transgenic lines contained at least one intact copy of the CoYMV-driven expression cassette (Fig. 1c) and an estimated number of transgene loci ranging between one and four (Fig. 1b). Moreover, Northern blot

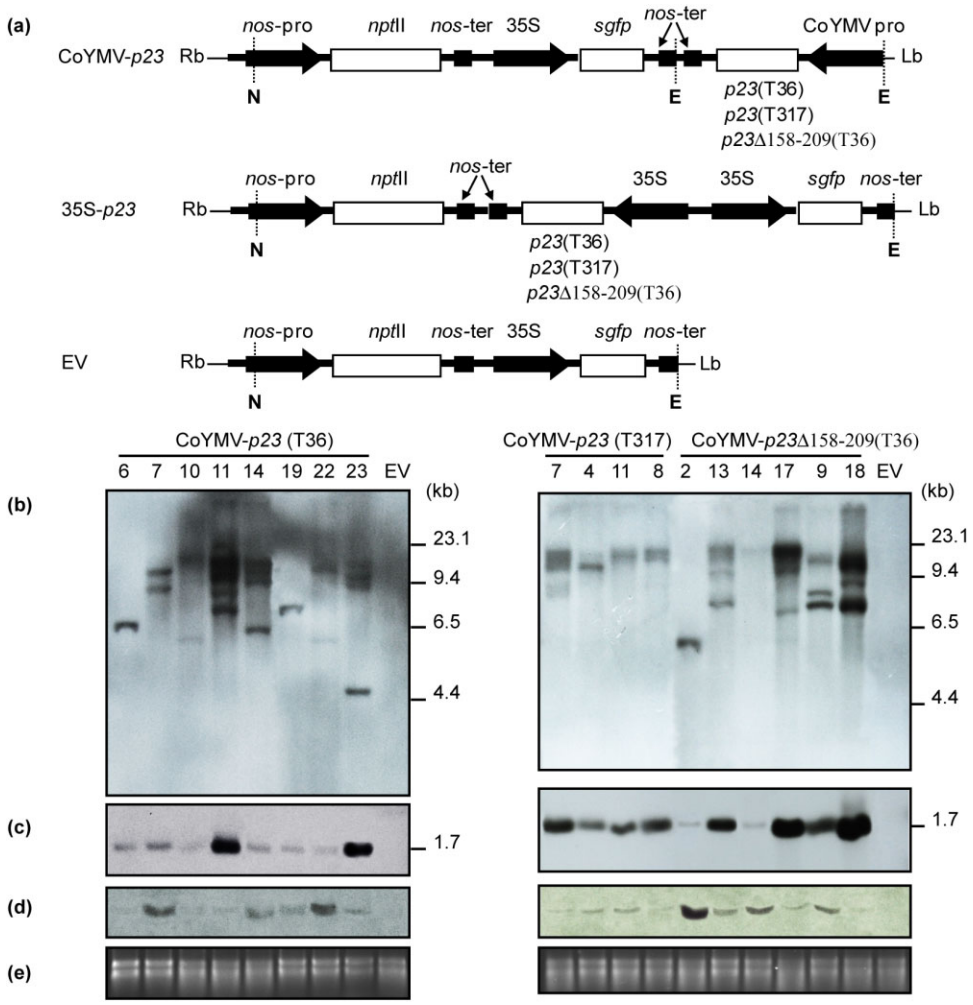

Fig. 1 Diagram of the T-DNA from the binary vectors CoYMV-p23 and 35S-p23, and Southern/Northern blot analyses from transgenic Mexican lime. (a) Diagram of the T-DNA from the binary vectors CoYMV-*p23* and 35S-*p23* carrying the *p23*(T36), *p23*(T317) or *p23Δ158–209*(T36) cassette under the control of the phloem-specific promoter from *Commelina yellow mottle virus* (CoYMV-pro) and the nopaline synthase terminator (*nos*-ter), and the constitutive 35S promoter from cauliflower mosaic virus (35S-pro) and *nos*-ter, respectively. These cassettes were flanked by the neomycin phosphotransferase II gene (*npt*II) between the *nos* promoter (*nos*-pro) and *nos*-ter, and by the green fluorescent protein gene (s*gfp*) between 35S-pro and *nos*-ter. The binary vector pBin19-s*gfp* was used as an empty vector (EV) control. Transcription orientation for each cassette is indicated by arrows. N and E denote *Nhe*I and *Eco*RI restriction sites, respectively. (b–e) Southern and Northern blot hybridization of nucleic acid preparations from lime plants transformed with the CoYMV-*p23*(T36) construct (lines 6, 7, 10, 11, 14, 19, 22 and 23), CoYMV-*p23*(T317) construct (lines 7, 4, 11 and 8), CoYMV-*p23Δ158–209*(T36) construct (lines 2, 13, 14, 17, 9 and 18) and empty vector (EV). DNA was digested with *Nhe*I (b), which cuts once the T-DNA, or with *Eco*RI (c), which excises the CoYMV-*p23* expression cassette. The size of the DNA markers is indicated on the right. (d) Total RNA extracted from transgenic plants was separated by electrophoresis in a formaldehyde-containing agarose gel, and transferred to a nylon membrane. (e) Ethidium bromide staining of the RNA gel showing that equivalent amounts of RNA were loaded in the different lanes. (b–d) Membranes were probed with a digoxigenin-labelled fragment of the *p23*-coding region.

analysis showed variable transgene expression depending on the line, with an inverse but not strict correlation being observed between the transgene loci number and transcript expression (Fig. 1d,e). Five propagations were prepared from each of the selected CoYMV-*p23* and EV transgenic lines, as well as from selected 35S-*p23* transgenic lines of Mexican lime, generated and characterized previously, expressing p23 under the control of the constitutive promoter 35S from cauliflower mosaic virus (CaMV) (Fagoaga *et al*., 2005; Ghorbel *et al*., 2001; Ruiz-Ruiz *et al*., 2013). CTV-infected non-transformed plants were also propagated in parallel and used as controls.

About 3–6 months after propagation in the glasshouse, transgenic Mexican lime harbouring the CoYMV-*p23*(T36), CoYMV-*p23Δ158–209*(T36) or CoYMV-*p23*(T317) cassette displayed

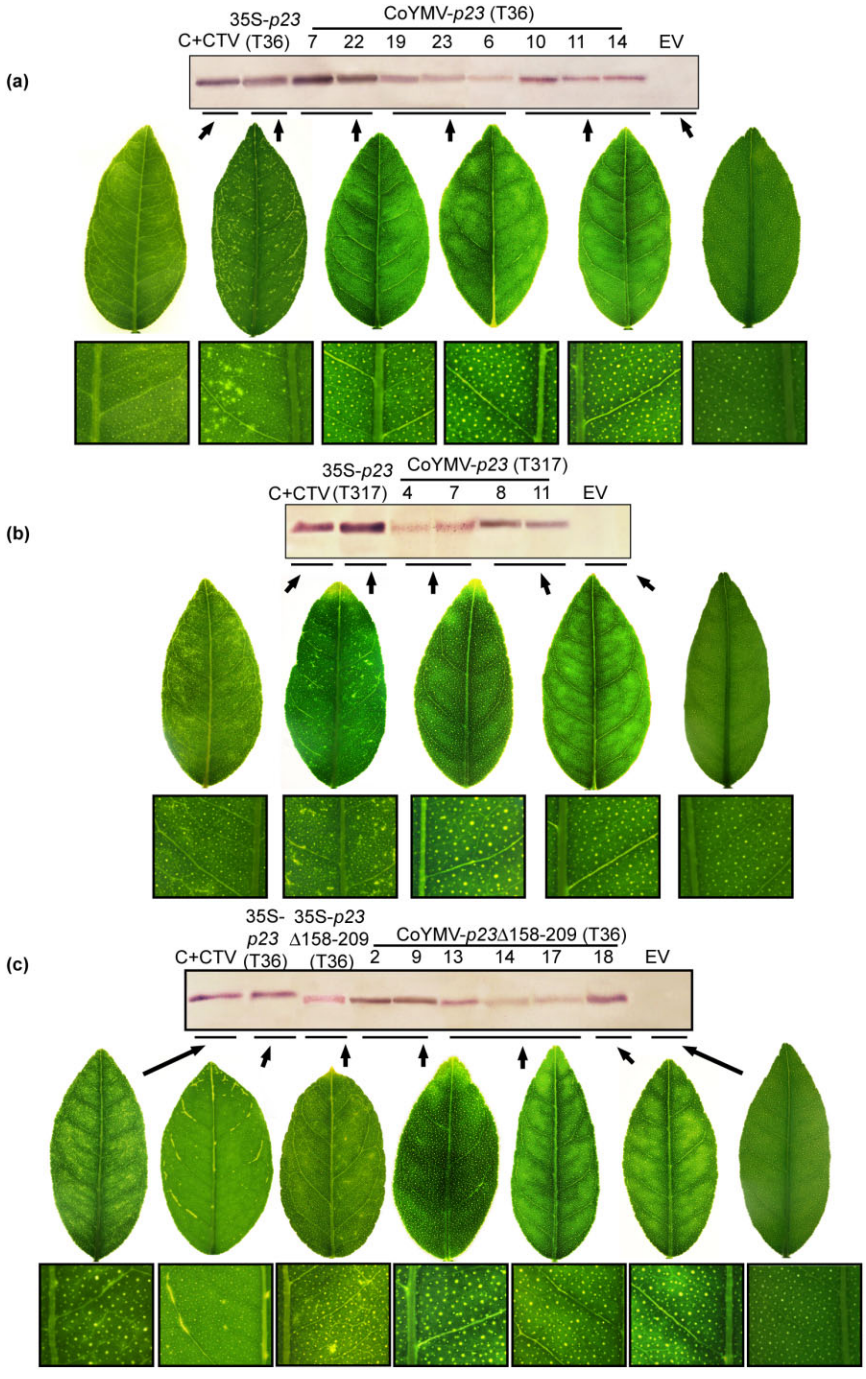

Fig. 2 Accumulation of p23 and vein clearing symptoms in developing leaves from transgenic Mexican limes. Western blot analysis of protein preparations separated by sodium dodecylsulfate-polyacrylamide gel electrophoresis (SDS-PAGE) (12%) and probed with a specific antibody of: (a) p23 from *Citrus tristeza virus* (CTV) T36, (b) p23 from CTV T317 and (c) p23Δ158–209 from CTV T36. Vein clearing shown by leaves of Mexican lime transformed with: (a) CoYMV-*p23*(T36), (b) CoYMV-*p23*(T317) and (c) CoYMV-*p23Δ158–209*(T36). Controls include non-transgenic Mexican limes infected with CTV T36 (C + CTV), and 35S-*p23*(T36) and empty vector (EV) transgenic plants. To better illustrate vein clearing, the magnification is shown below each leaf.

progressive vein clearing in developing leaves, in contrast with the asymptomatic phenotype exhibited by similar leaves from plants transformed with the EV cassette (Fig. 2). This phenotypic anomaly was essentially identical to the vein clearing induced by CTV T36 in non-transgenic plants of this host (Fig. 2; C + CTV lanes and corresponding leaf samples). All CoYMV-*p23* Mexican lime transformants accumulated detectable amounts of p23 or p23Δ158–209, unlike those plants carrying the EV construct, as revealed by Western blot analysis (Fig. 2). Moreover, the accumulation of p23 from CTV T36 or T317, or p23Δ158–209 from T36, in CoYMV-*p23*(T36), CoYMV-*p23*(T317) and CoYMV-*p23Δ158-209*(T36) transgenic plants, respectively, correlated positively with

the CTV-like vein clearing intensity. For example, lines CoYMV-*p23*(T36)-7 and CoYMV-*p23*(T36)-22 (Fig. 2a), lines CoYMV-*p23*(T317)-8 and CoYMV-*p23*(T317)-11 (Fig. 2b) and lines CoYMV-*p23Δ158–209*(T36)-2 and CoYMV-*p23Δ158–209*(T36)-9 (Fig. 2c) displayed pronounced vein clearing and high p23 accumulation, whereas lines CoYMV-*p23*(T36)-23 and CoYMV-*p23*(T36)-6 (Fig. 2a), lines CoYMV-*p23*(T317)-4 and CoYMV-*p23*(T317)-7 (Fig. 2b) and lines CoYMV-*p23Δ158–209*(T36)-14 and CoYMV-*p23Δ158–209*(T36)-17 (Fig. 2c) showed milder vein clearing and accumulated low to moderate levels of p23 (Fig. 2). Therefore, the phloem-specific expression of p23 from the mild strain T317 induced vein clearing in Mexican lime similar to that induced by the severe strain T36, with the intensity being correlated with p23 accumulation irrespective of the source strain, as reported previously for the constitutive expression of p23 from both strains (Fagoaga *et al*., 2005).

Mexican lime transformed with CoYMV-*p23* constructs develops stem pitting and vein necrosis similar to that induced by the severe CTV strain T36 in non-transformed plants

Six to twelve months after propagation in the glasshouse, transgenic plants CoYMV-*p23*(T36) and CoYMV-*p23Δ158-209*(T36) exhibited stem pitting similar to that of transgenic plants 35S-*p23*(T36) (Ghorbel *et al*., 2001) and 35S-*p23Δ158-209*(T36) (Ruiz-Ruiz *et al*., 2013) (Fig. 3a). This phenotypic aberration was also very similar to the stem pitting induced by CTV T36 in

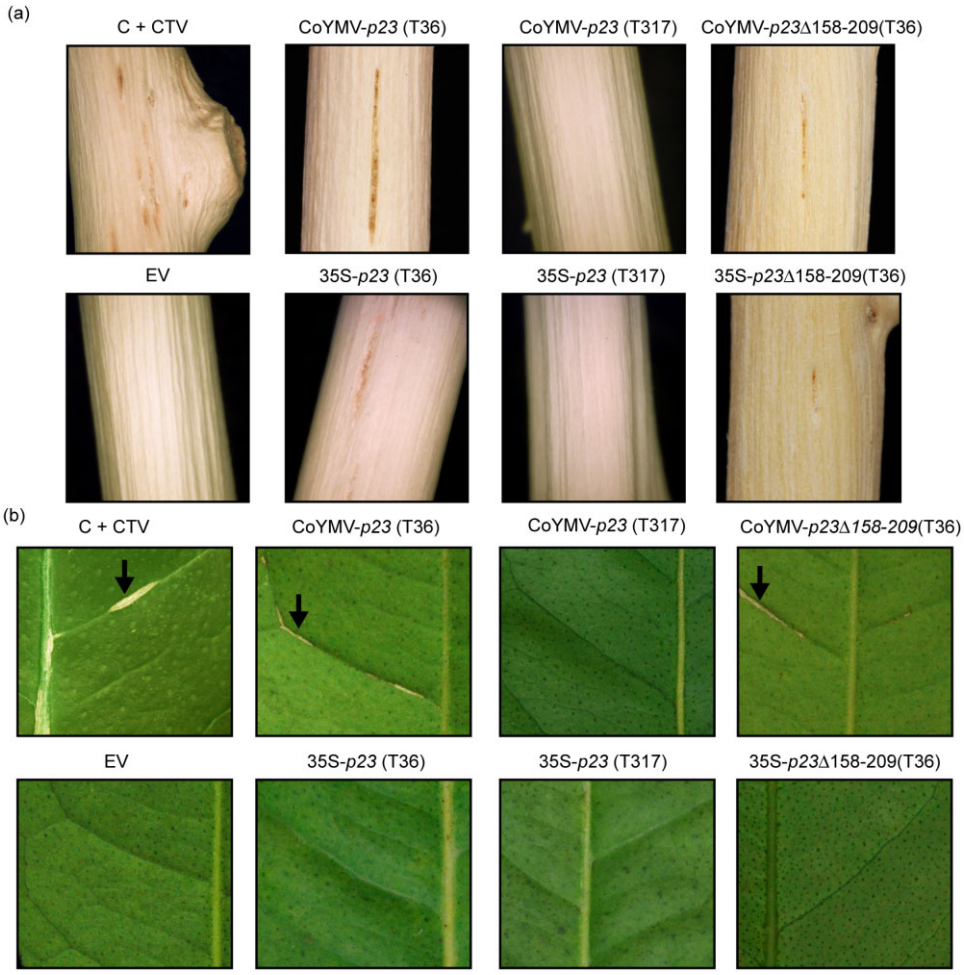

Fig. 3 Stem pitting (a) and vein necrosis (b) *Citrus tristeza virus* (CTV)-like symptoms exhibited by CoYMV-*p23*(T36) and CoYMV-*p23Δ158–209*(T36) transgenic Mexican limes. Neither stem pitting nor vein necrosis was detected in CoYMV-*p23*(T317) transgenic plants (a, b). Controls include non-transgenic Mexican limes inoculated with CTV T36 (C + CTV), and 35S-*p23*(T36), 35S-*p23Δ158–209*(T36), 35S-*p23*(T317) and empty vector (EV) transgenic plants.

non-transgenic Mexican lime, although pitting was more pronounced and extended in the latter case (Fig. 3a). The stem pitting intensity was comparable in all transgenic plants expressing the different versions of p23 and p23Δ158-209, irrespective of their accumulation levels (data not shown). This lack of correlation is possibly associated with the weak stem pitting induced by both p23(T36) versions in transgenic Mexican lime (Fig. 3a). Conversely, CoYMV-*p23*(T317) transgenic plants accumulating p23 did not show stem pitting at any developmental stage, behaving in a similar manner to the EV transgenic controls (Fig. 3a). As 35S-*p23*(T317) transgenic plants did not display stem pitting (Fig. 3a; Fagoaga *et al*., 2005), our results indicate that this symptom depends on the p23 source rather than on its accumulation level. In non-transformed Mexican lime, strain T317 causes only mild vein clearing (Moreno *et al*., 1993).

After 1 year in the glasshouse, transgenic plants CoYMV-*p23*(T36) and CoYMV-*p23Δ158–209*(T36) exhibited vein necrosis on the lower surface of mature leaves, resembling vein corking induced in non-transformed Mexican lime by severe CTV strains, including T36, although such vein corking usually occurs on the upper leaf surface (Fig. 3b). Moreover, the intensity of vein necrosis generally paralleled the accumulation of p23. For example, while lines CoYMV-*p23*(T36)-7 and CoYMV-*p23*(T36)-11 and lines CoYMV-*p23Δ158–209*(T36)-2 and CoYMV-*p23Δ158–209*(T36)-9 displayed marked vein necrosis and accumulated high to moderate levels of p23, lines CoYMV-*p23*(T36)-6 and CoYMV-*p23*(T36)-23 and lines CoYMV-*p23Δ158–209*(T36)-14 and CoYMV-*p23Δ158–209*(T36)-17 showed mild vein necrosis and lower p23 accumulation (Fig. 2a,c; Fig. 3b; data not shown). In contrast, vein necrosis was absent in transgenic plants CoYMV-*p23*(T317), as well as in transgenic plants 35S-*p23*(T36), 35S-*p23Δ158–209*(T36), 35S-*p23*(T317) and EV (Fig. 3b), indicating that this aberration is exclusively associated with the phloem-specific expression of p23 from T36. Therefore, the most severe phenotypic effects in Mexican lime transformants (stem pitting and vein necrosis) seem to be related to the source of p23 and, more specifically, to its N-terminal fragment of 157 amino acids. Comparison of the predicted amino acid sequence of p23 from 18 CTV isolates of different pathogenicity showed three regions (demarcated by positions 24–29, 50–54 and 78–80) in which mild CTV isolates, but not other isolates, had the same sequence (Sambade *et al*., 2003). Interestingly, these regions include most amino acid differences between p23 from T317 and T36 (or its Δ158–209 version). Regions 50–54 and 78–80 form part of two domains that include several basic residues (positions 50–67) and a putative zinc finger motif (positions 68–86), which are crucial for the RNA-binding activity of p23 (López *et al*., 2000) and its nucleolar localization (Ruiz-Ruiz *et al*., 2013). Altogether, these results support the involvement of the p23 fragment, encompassing the N-terminal 157 amino acids, in the induction of the CTV-like stem pitting and vein necrosis.

Aberrations induced by phloem-specific expression of p23 or its N-terminal fragment of 157 amino acids in Mexican lime are histologically similar to those induced by CTV in non-transformed plants

To corroborate that vein clearing induced by the phloem-specific expression of p23 from T317, and vein clearing and necrosis induced by the phloem-specific expression of p23 and p23Δ158–209 from CTV T36 in Mexican lime mimic the symptoms induced by the corresponding CTV strain in non-transformed plants, we examined cross-sections of leaf veins from: (i) transgenic plants CoYMV-*p23*(T36), CoYMV-*p23*(T317) and CoYMV-*p23Δ158–209*(T36); (ii) transgenic plants 35S-*p23*(T36), 35S-*p23*(T317), 35S-*p23Δ158–209*(T36) and EV; and (iii) non-transformed controls infected with CTV T36 (C + CTV).

Examination by light microscopy showed that the xylem cap, phloem and phloem fibres were fully differentiated in EV control veins, with air spaces on each side of the vein (Fig. 4a,i). However, vein clearing areas in CTV-infected plants (C + CTV) showed hypertrophied cells developed from the primary phloem fibres, which occluded the air spaces normally found around veins (Fig. 4b). Differentiation failed to occur, and so veins lacked the caps of primary phloem fibres and sheath cells (Schneider, 1959). Vein clearing areas from CoYMV-*p23*(T36), CoYMV-*p23*(T317), CoYMV-*p23Δ158–209*(T36) (Fig. 4f,g,h, respectively) and 35S-*p23*(T36), 35S-*p23*(T317), 35S-*p23Δ158–209*(T36) (Fig. 4c,d,e, respectively) leaves displayed obliterated cells in the phloem cap and hypertrophied cells occluding part of the air spaces found normally around the veins. Therefore, the vein clearing shown by CoYMV-*p23* plants was histologically indistinguishable from that exhibited by 35S-*p23* plants, and similar to, albeit less intense than, the vein clearing induced by CTV T36 in the non-transformed counterparts.

Cross-sections from necrotic veins in CoYMV-*p23*(T36) (Fig. 4k) and CoYMV-*p23Δ158–209*(T36) plants (Fig. 4l) displayed excessive phloem formation displacing phloem fibres, and the phloem cap showed obliterated cells as well as collapsed and necrotic areas. Corking areas from C + CTV leaves exhibited a disorganized tissue, with phloem over-formation, obliterated cells, collapsed and necrotic areas, and a lack of phloem fibres (Fig. 4j). These results indicate that vein necrosis in CoYMV-*p23*(T36) and CoYMV-*p23Δ158–209*(T36) transgenic lime strongly resembles the vein corking induced by CTV in this host, but with more pronounced tissue disorganization and necrosis in the second case (Fig. 4j,k,l).

How does phloem-specific expression of p23 induce CTV-like symptoms in Mexican lime?

The transgenic expression of p23 in Mexican lime, controlled by a phloem-specific promoter, mimics virus-induced symptoms more

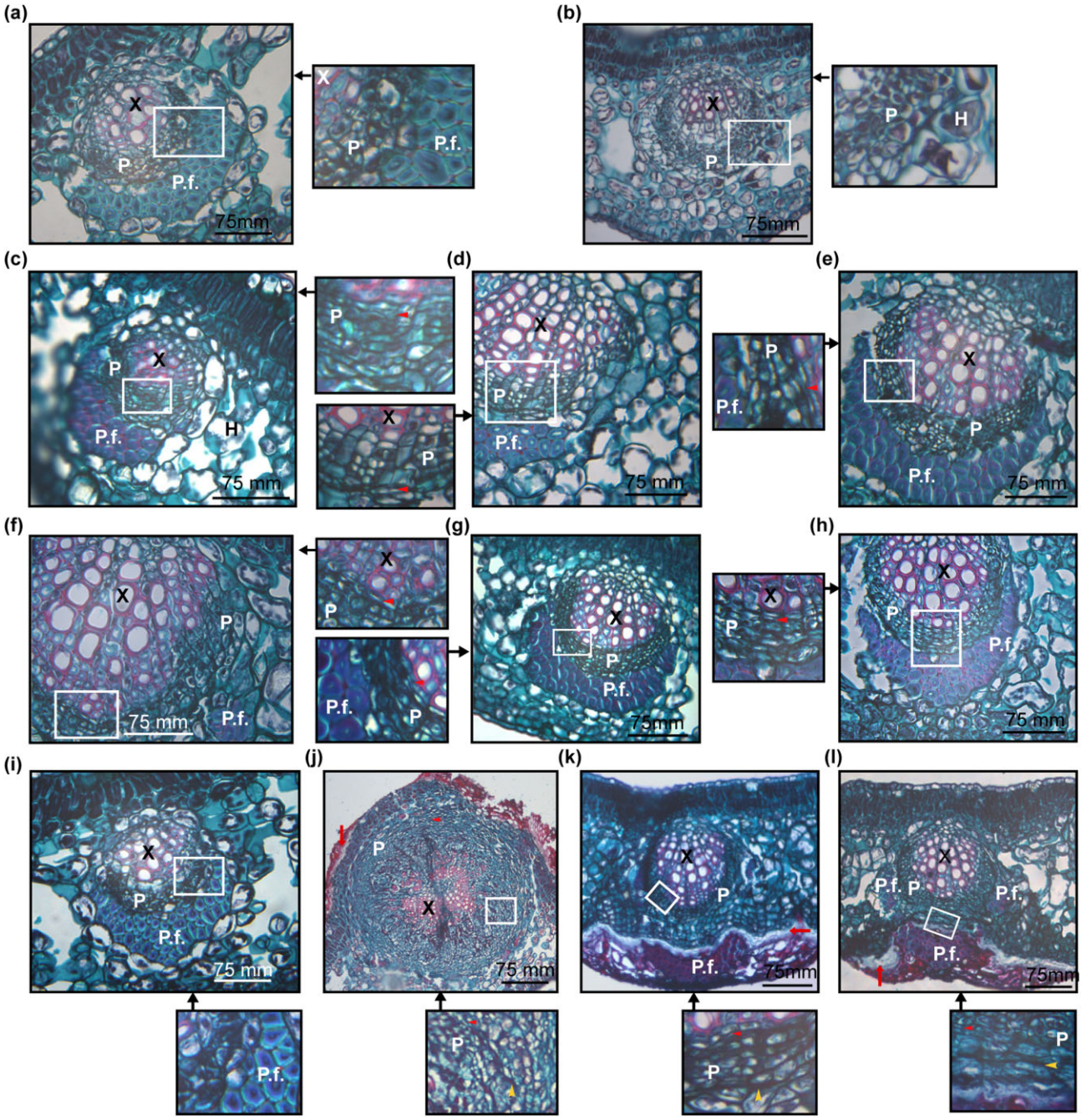

Fig. 4 Cross-sections of representative leaf veins from CoYMV-*p23*(T36), CoYMV-*p23Δ158–209*(T36), 35S-*p23*(T36), 35S-*p23*(T317), 35S-*p23Δ158–209*(T36) and empty vector (EV) transgenic limes and non-transgenic limes infected with CTV T36 (C + CTV), stained with a combination of safranin O and Fast Green FCI. (a, i) Healthy leaves from non-inoculated 6- and 12-month-old EV transgenic plants, respectively. (b) Vein clearing area from a non-transgenic lime infected with CTV T36 (C + CTV). (c–e) Vein clearing area from 35S-*p23*(T36) (c), 35S-*p23*(T317) (d) and 35S-*p23Δ158–209*(T36) (e) transgenic plants. (f–h) Vein clearing area from CoYMV-*p23*(T36) (f), CoYMV-*p23*(T317) (g) and CoYMV-*p23Δ158–209*(T36) (h) transgenic plants. (j) Vein corking area from a non-transgenic lime infected with CTV T36 (C + CTV). (k) Necrotic vein from a CoYMV-*p23*(T36) transgenic plant. (l) Necrotic vein from a CoYMV-*p23Δ158–209*(T36) transgenic plant. The white rectangles in (a–l) are shown at higher magnification in adjacent panels indicated by black arrows. H, hypertrophic cells; P, phloem; P.f., phloem fibre; X, xylem; obliterated cells, collapsed areas and necrotic areas are indicated by small red, yellow and long red arrows, respectively.

accurately than when expressed from a constitutive promoter. In particular, the phloem-specific expression of p23(T36) and p23Δ158–209(T36) in Mexican lime induced, in addition to vein clearing, vein necrosis and stem pitting very similar to that induced by T36 in non-transformed plants. Similarly, the phloem-specific expression of p23(T317) induced vein clearing, but not vein necrosis or stem pitting, recapitulating the symptoms induced by T317 in non-transformed plants. In contrast, the constitutive expression of p23 (from T36 or T317) failed to induce vein necrosis, but resulted in chlorotic pinpoints, apical necrosis and mature leaf epinasty (not observed in natural CTV infections) (Fagoaga *et al*., 2005; Ghorbel *et al*., 2001). Therefore, these latter aberrations are probably associated with the ectopic accumulation of this protein in non-phloem cells, wherein CTV does not replicate and accumulate.

p23 has characteristics in common with other viral proteins, such as 2b from cucumoviruses and P0 from poleroviruses, which are pathogenicity determinants that induce developmental aberrations when expressed in transgenic plants (Bortolamiol *et al*., 2007; Ghorbel *et al*., 2001; Lewsey *et al*., 2007; Ruiz-Ruiz *et al*., 2013; this work), show nuclear/nucleolar localization (Fusaro *et al*., 2012; González *et al*., 2010; Ruiz-Ruiz *et al*., 2013) and function as RSSs in *Nicotiana* spp. (Lu *et al*., 2004; Ruiz-Ruiz *et al*., 2013; Voinnet *et al*., 1999). Like 2b and P0, p23 may cause symptoms by targeting ARGONAUTE (AGO) proteins for degradation (Bortolamiol *et al*., 2007), by preventing the *de novo* assembly of the RNA-induced silencing complex (RISC) (Baumberger *et al*., 2007; Duan *et al*., 2012; Zhang *et al*., 2006) or by promoting host epigenetic modifications via the transport of small RNAs to the nucleus (Kanazawa *et al*., 2011). As the region comprising the N-terminal 157 amino acids of p23 is responsible (at least in part) for symptoms in Mexican lime, and as p23Δ158–209 lacks the ability of RSS in *N. benthamiana* (Ruiz-Ruiz *et al*., 2013), the pathogenicity of p23 seems to be independent of its RSS activity (although the situation may not be the same when p23 is expressed in its natural virus–host context), and is possibly linked to its major subcellular localization (as well as that of p23Δ158–209) in the nucleolus and/or plasmodesmata (Ruiz-Ruiz *et al*., 2013).

To obtain a deeper insight into the mechanisms involved, we examined the mRNA accumulation levels of some candidate genes whose expression may be altered by p23. When compared with the non-transformed control (C), we were unable to detect significant differences in the mRNA levels of the citrus homologue of *AGO1* from *A. thaliana* in midribs from 35S-*p23*(T36), 35S-*p23Δ158–209*(T36), CoYMV-*p23*(T36), CoYMV-*p23Δ158–209*(T36) and CoYMV-*p23*(T317) developing leaves (Fig. 5a). Significant up-regulation of the citrus *AGO1* mRNA was only observed in midribs from non-transformed controls infected with CTV T318A (C + CTV 318A), a severe CTV isolate, but not in those infected with CTV T36 (C + CTV T36) (Fig. 5a). Therefore, symptoms resulting from CTV T36 infection, and, in particular, the aberrations induced by transgenic expression of p23, do not appear to be associated with alterations in the levels of *AGO1* mRNA. As CTV T318A infection affects the relative abundance of many citrus miRNAs, including miRNA167 (Ruiz-Ruiz *et al*., 2011), which regulates AUXIN RESPONSE FACTOR 8 (ARF8), misregulation of *ARF8* was also tested. CTV T318A infection and the constitutive over-expression of *p23*(T36) induced in midribs increased accumulation of the citrus *ARF8* mRNA within a 1.5–2-fold range (Fig. 5b). A similar *ARF8* up-regulation range underlies most of the developmental abnormalities caused by the expression of three unrelated RSSs in *A. thaliana*, in both transgenic and virus infection contexts (Jay *et al*., 2011). Although no correlation was found between p23 accumulation and *ARF8* expression in midribs from CTV-infected or p23 transgenic Mexican lime, the finding that plants with the earliest and most intense vein clearing symptoms or symptom-like aberrations [C + CTV T318A and 35S-*p23*(T36)] were those with higher *ARF8* mRNA levels suggests the association of *ARF8* over-expression with the onset of this phenotype.

Alternatively, p23 may interact with host factors unrelated to RNA silencing pathways, as illustrated by the interactions of the replicase protein from *Tobacco mosaic virus* with the auxin/indole 3-acetic acid (Aux/IAA) protein PAP1/IAA26 (Padmanabhan *et al*., 2005), CMV 2b with catalase 3 (Inaba *et al*., 2011) and p12 from a carlavirus with the promoter of a gene that encodes a transcription factor (*upp-L*, up-regulated by p12) causing hyperplasia on induction (Lukhovitskaya *et al*., 2013). However, attempts to link the accumulation of p23 from T36 or T317 with that of the mRNAs from the citrus homologues of the *catalase 3* or *upp-L* genes from *A. thaliana* were unsuccessful (Fig. 5c,d). These genes were up-regulated only in midribs from plants infected with CTV T318A, most likely as an indirect effect of the severity of this isolate, which induces drastic transcriptomic alterations in Mexican lime (Gandía *et al*., 2007), and not from specific interactions of its p23 with the tested targets.

EXPERIMENTAL PROCEDURES

Recombinant vectors

The CoYMV promoter and the binary vector pGPTV harbouring the CoYMV promoter were kindly provided by Dr Neil Olszewski (University of Minnesota, St Paul, MN, USA) and Dr Biao Ding (Ohio State University, Columbus, OH, USA), respectively. The DNA fragment containing the CoYMV promoter and the *nopaline synthase* terminator (*nos*-ter) was excised with *Sal*I and *Eco*RI from plasmid pGPTV and inserted into the respective restriction sites of plasmid pTZ57R (Fermentas GmbH, St. Leon-Rot, Germany) to generate the intermediate plasmid pTZ57R-CoYMV. Polymerase chain reaction (PCR) amplification of the *p23* gene from CTV-T36 (or a deletion mutant thereof) and CTV-T317 from the respective pMOG-*p23*-T36 (Ghorbel *et al*., 2001), pMOG-*p23Δ158–209*(T36) (Ruiz-Ruiz *et al*.,

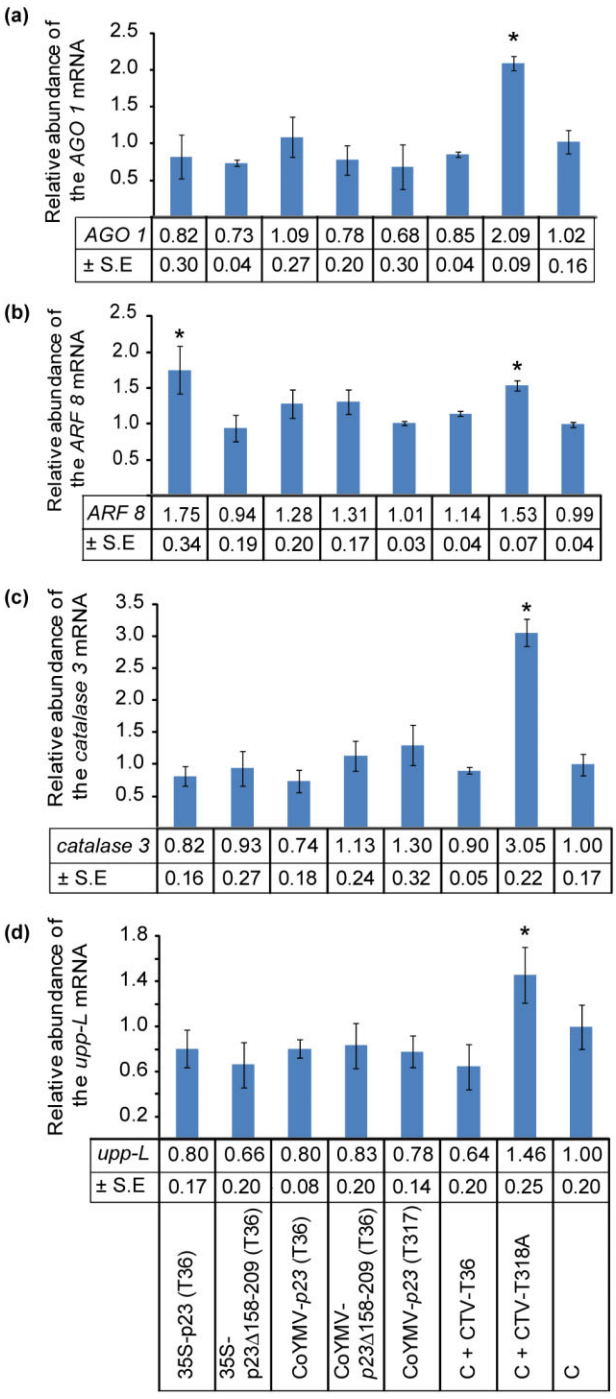

Fig. 5 Accumulation levels, assessed by real-time quantitative reverse transcription-polymerase chain reaction (qRT-PCR), of the mRNAs of the citrus homologues of *ARGONAUTE 1* (*AGO1*) (a), *AUXIN RESPONSE FACTOR 8* (*ARF8*) (b), *catalase 3* (c) and *upp-L* (d) in midribs of developing leaves (3–4 cm) from 35S-*p23*(T36), 35S-*p23Δ158–209*(T36), CoYMV-*p23*(T36), CoYMV-*p23Δ158–209*(T36) and CoYMV-*p23*(T317) transgenic Mexican limes, from non-transgenic Mexican limes infected with CTV T36 (C + CTV-T36) or CTV T318A (C + CTV-T318A), and from non-transgenic non-infected Mexican limes (C). Relative mRNA levels were normalized to those of the citrus actin mRNA. Three independent biological replicates from a pool of midribs from three independent plants from three independent transgenic events per construct, or a pool of six plant replicates in the CTV-infected and non-infected control plants, were used. Means ± standard error (SE) were calculated and significant differences from C at $P < 0.05$ are indicated with an asterisk.

2013) and pMOG-*p23*-T317 (Fagoaga *et al*., 2005) plasmids was performed with *Pfu* DNA polymerase (Stratagene, La Jolla, CA, USA) using the sense and antisense primers RF-167 (5'-CTTggatccATGGATAATA CTAGCGG-3') and RF-168 (5'-CTTggatccTCAGATGAAGTGGTGTTC-3'), respectively, containing a *Bam*HI restriction site (in lowercase letters) to facilitate cloning. The pMOG-*p23*-T36 plasmid was also used to generate the deletion mutant pMOG-*p23Δ158–209*(T36), in which the nucleotide guanine at position 472 was replaced by a thymine, resulting in a stop codon immediately after amino acid 157 (thus deleting the C-terminal 51 amino acids from p23 without affecting the zinc finger or any of the three flanking basic motifs). For this purpose, the pMOG-*p23*-T36 plasmid was PCR amplified with *Pfu* DNA polymerase using the pair of divergent primers of opposite polarity RF-353 (5'-CATCGGGTGTCTACGAGCCAGTC-3') and RF-354 (5'-CGTTCTCCGtAAGAAACTCCGG-3'), in which the lowercase letter indicates nucleotide substitution, to yield pMOG-*p23Δ158–209*(T36).

After *Bam*HI digestion, the PCR-amplified fragments were inserted between the CoYMV promoter and *nos*-ter by ligation in the *Bam*HI-digested pTZ57R-CoYMV plasmid, generating the intermediate plasmids pTZ57R-CoYMV-*p23*(T36), pTZ57R-CoYMV-*p23*(T317) and pTZ57R-CoYMV-*p23Δ158–209*(T36). *Eco*RI restriction sites were inserted at the 5' end of the CoYMV promoter and at the 3' end of *nos*-ter in the three constructions by PCR amplification using the primers Phloem-D-Eco (5'-CTTgaattcGGTATCGATTTCTTAGGGGC-3') and Phloem-R-Eco (5'-CTTga attcCCGATCTAGTAACATAGATG-3'), with the restriction site indicated in lowercase letters. The CoYMV-*p23* cassettes were digested with *Eco*RI and inserted into the unique *Eco*RI site of the binary vector pBin19-*sgfp* (Chiu *et al*., 1996), adjacent to the *nos*-pro/*nptII*/*nos*-ter and 35S-pro/*sgfp*/*nos*-ter cassettes (Fig. 1a). The plasmid pBin19-s*gfp* was used as an EV control. The construction of pBin19-35S-*p23*(T36), pBin19-35S-*p23*(T317) and pBin19-35S-*p23Δ158–209*(T36), with the *p23* transgenes controlled by the 35S promoter of CaMV, have been described in Ghorbel *et al*. (2001), Fagoaga *et al*. (2005) and Ruiz-Ruiz *et al*. (2013), respectively. Binary vectors were electroporated into the disarmed *Agrobacterium tumefaciens* strain EHA105, which was used to transform Mexican lime, as described previously (Ghorbel *et al*., 2001).

Transgenic plant generation

The selection of transformants was performed on a culture medium containing kanamycin (100 mg/L), and the regenerated shoots were examined under a Leica MZ 16 stereomicroscope equipped with a GFP-Plus Fluorescence module (Leica Microsystems, Wetzlar, Germany). Shoots exhibiting bright green fluorescence were excised and grafted *in vitro* on Troyer citrange [*C. sinensis* (L.) Osb. × *Poncirus trifoliata* (L.) Raf.] seedlings (Peña and Navarro, 1999; Soler *et al*., 2012). The integrity of the *p23* transgenes

was assessed by PCR with appropriate primers. PCR-positive plantlets were grafted onto vigorous 6-month-old Carrizo citrange seedlings and grown in a glasshouse at 24–26 °C/16–18 °C (day/night), 60%–80% relative humidity and natural light. Buds from transgenic Mexican lime lines harbouring the EV, CoYMV-*p23* or CaMV 35S-*p23* cassette (Fagoaga *et al*., 2005; Ghorbel *et al*., 2001; Ruiz-Ruiz *et al*., 2013), or from non-transgenic control plants infected with CTV T36 or CTV T317, were propagated on vigorous Carrizo citrange rootstocks in parallel. Plants were grown in individual 2.5-L pots containing a mixture of 55% sphagnum peat and 45% siliceous sand, and were fertilized weekly.

The growth and symptom expression of transgenic and non-transgenic CTV-infected Mexican lime plants were periodically observed for at least 3 years. Developmental aberrations in transgenic lines and CTV-induced symptoms in infected plants were photographed with a Nikon D80 camera (Nikon Corporation, Tokyo, Japan) and specific details from leaves and peeled branches were photographed with a Leica MZ 16 stereomicroscope equipped with a Leica DFC490 camera (Leica Microsystems).

Southern, Northern and Western blot analyses

To analyse the integrity and number of loci of the CoYMV-*p23* expression cassettes in Mexican lime plants, Southern blot hybridization analysis was performed. DNA aliquots (15 μg) extracted from leaves (Dellaporta *et al*., 1983) were digested with *Eco*RI, which excises the expression cassettes (Fig. 1a), or with *Nhe*I, which cuts once the T-DNA (Fig. 1a). After agarose gel electrophoresis, the DNA was blotted onto positively charged nylon membranes, fixed by UV irradiation, probed with a digoxigenin (DIG)-labelled cDNA fragment of the *p23* coding region prepared by PCR according to the manufacturer's instructions (Boehringer Mannheim GmbH, Mannheim, Germany) and detected using the chemiluminescent CSPD substrate (Roche Diagnostics Corporation, Indianapolis, IN, USA). For the detection of transgene-derived transcripts, Northern blot hybridization analysis was performed. Total RNA from leaf midribs of transgenic plants was extracted with buffer-saturated phenol and fractionated with 2 M LiCl (Carpenter and Simon, 1998). Aliquots (20 μg) of the insoluble RNA fraction were electrophoresed in 1% agarose gels containing formaldehyde, blotted onto nylon membranes, fixed by UV irradiation and probed with a digoxigenin-labelled cDNA fragment of the *p23* coding region according to the manufacturer's instructions (Boehringer-Mannheim GmbH) and detected by chemiluminescence with the CSPD substrate (Roche Diagnostics Corporation).

The accumulation of p23 and p23Δ158–209 proteins in transgenic Mexican lime plants was tested by Western blot analysis. Total protein was extracted from leaf midribs with 100 mM Tris-HCl, pH 6.8, containing 0.3% β-mercaptoethanol and 1 mM phenyl-methyl-sulfonyl fluoride, and quantified with the Protein Assay Dye Reagent (Bio-Rad, Hercules, CA, USA) using bovine serum albumin as a standard (Bradford, 1976). Aliquots (50 μg) were electrophoresed in sodium dodecylsulfate-polyacrylamide gels (12%), electroblotted onto poly(vinylidene difluoride) (PVDF) membranes and probed with a polyclonal antibody (1 μg/mL) against p23Δ50–86 (Ruiz-Ruiz *et al*., 2013). Binding of the antibody was detected with goat anti-rabbit immunoglobulin G (IgG) conjugated with alkaline phosphatase (Sigma-Aldrich, St Louis, MO, USA) and visualized with 5-bromo-4-chloro-3-indolyl phosphate/nitroblue tetrazolium SIGMA *FAST*™ BCIP/NBT (Sigma-Aldrich). Extracts from leaf midribs of transgenic Mexican lime plants carrying the EV control construct and from non-transgenic Mexican limes infected with CTV (C + CTV) were used as negative and positive controls, respectively.

Histological analysis

Leaf pieces of approximately 1 × 0.5 cm^2, including minor veins and midribs, were collected from areas with vein clearing or vein necrosis aberrations from CoYMV-*p23*(T36)-, CoYMV-*p23Δ158–209*(T36) and CoYMV-*p23*(T317) transgenic Mexican lime plants, their 35S-*p23* counterparts, symptomatic areas of non-transgenic CTV-infected Mexican limes and similar asymptomatic areas of non-infected EV control plants.

Leaf samples were fixed in FAA solution (0.5: 9 :0.5 v/v/v of formaldehyde, ethanol and acetic acid) for 15 days and dehydrated through a series of ethanol/tertiary butyl alcohol solutions (Jensen, 1962). After embedding in histosec® pastilles (solidification point, 56–58 °C) (Merck, Whitehouse Station, NJ, USA), 10-μm-thick cross-sections of leaf veins were obtained with a rotary microtome (Jung, Heidelberg, Germany). Sections were stained with a combination of safranin O (Merck) (lignified cellular walls stain red) and Fast Green FCI (Sigma-Aldrich) (cellulose stains blue–green), mounted with Canada balsam (Merck) (Jensen, 1962; Román *et al*., 2004) and examined and photographed with a Leica DMLS microscope equipped with a Leica DFC490 digital camera.

Quantitative reverse transcription-polymerase chain reaction (qRT-PCR) analysis

Midribs of developing leaves (3–4 cm) from 35S-*p23*(T36) (lines 1, 35 and 42), 35S-*p23Δ158–209*(T36) (lines 2, 3 and 5), CoYMV-*p23*(T36) (lines 7, 19 and 22), CoYMV-*p23Δ158–209*(T36) (lines 2, 9 and 18) and CoYMV-*p23*(T317) (lines 7, 8 and 11) transgenic Mexican limes, from non-transgenic Mexican limes infected with CTV T36 (C + CTV T36) or CTV T318A (C + CTV T318A) and from non-transgenic non-infected Mexican limes (C) were used for real-time qRT-PCR. RNA was extracted and cleaned with the RNeasy Plant Mini kit (Qiagen, Hilden, Germany), and then treated with DNase I (Rnase-Free DNase Set; Qiagen) following the manufacturer's instructions. RNA was quantified using a Nanodrop spectrophotometer (NanoDrop 2000C; Thermo Fisher Scientific, Waltham, MA, USA).

The mRNA levels of the selected citrus homologues of *AGO1*, *ARF8*, *catalase 3* and *upp-L*, with sequences retrieved from the database of the *Citrus sinensis* Annotation Project (http://citrus.hzau.edu.cn/orange/index.php), were estimated by real-time qRT-PCR using the SYBR Green assay and the Light-Cycler 480 System (Roche Diagnostics Corporation) equipped with LightCycler 480 version 1.5 software. The primers used were: AGO1.F (5'-CAAATCACTTTATGGTGCAAC-3') and AGO1.R (5'-TCTTCATACCATCATAGGCAG-3'), amplifying a fragment of 125 nucleotides from Cs7g17970; ARF8.F (5'-TCATGATGCACTTCAGATTCG-3') and ARF8.R (5'-CAGCATGTTCTGCATAGGACT-3'), amplifying a fragment of 142 nucleotides from Cs6g16030.7; Cat3.R (5'-GGACCCAACTACTTG ATGCTT-3') and Cat3.R (5'-TGGGATATCTCTCAGCATGAC-3'), amplifying a fragment of 154 nucleotides from Cs3g27280.4; and upp-L.F (5'-CAAAGCTTGAGCTCTCTCTCT-3') and upp-L.R (5'-GCTGCCATTTTTTTCA CTATT-3'), amplifying a fragment of 114 nucleotides from ABW97699.1 (GenBank annotation). Primers were designed with the Oligo primer analysis software 6.65.

A two-step reverse RT-PCR was carried out. First-strand cDNA was synthesized from 1 μg of total RNA using SuperScript II Reverse Transcriptase (Invitrogen, Carlsbad, CA, USA) following the manufacturer's protocol. cDNA samples (25 ng) were used for qPCR by adding 10 μL of LightCycler 480 DNA SYBR Green I Master 2X solution (Roche) and 300 nM of gene-specific primers in a total volume of 20 μL.

The qPCR cycling conditions included one step at 95 °C for 10 min, followed by 40 cycles of 95 °C for 10 s, 60 °C for 10 s and 72 °C for 20 s. Fluorescence intensity data were acquired during the 72 °C extension step, and the specificity of the reactions was verified by melting curve analysis. To transform fluorescence intensity measurements into relative mRNA levels, a four-fold dilution series of a cDNA preparation from Mexican lime leaf midribs was used as a standard curve, with each point being the mean value of at least three independent analyses. Relative mRNA levels were normalized to the mRNA of the citrus actin gene (GenBank accession no. CX289161) following the efficiency method (Pfaffl, 2001). The actin primers used were ACT-F (5'-CATGAAGTGT GATGTGGATATTAG-3') and ACT-R (5'-TGATTTCCTTGCTCATACGG-3'), amplifying a fragment of 106 nucleotides.

Induction values of one-fold were arbitrarily assigned to the control sample and the rest of the values were referred to this sample. The quantification of each transcript from each cDNA source was accomplished with at least three biological replicates using a pool of midribs from three plants from three different transgenic events per construct, or a pool of six plant replicates in CTV-infected and non-infected control plants. Mean ± standard error values were calculated.

ACKNOWLEDGEMENTS

We thank Dr B. Ding for providing a construct with the phloem-specific promoter from CoYMV, and J. E. Peris, J. Juárez and M. T. Gorris for their excellent technical assistance. N.S. was supported by a PhD fellowship from the Instituto Valenciano de Investigaciones Agrarias (IVIA). This research was supported by grants AGL2009-08052, co-financed by Fondo Europeo de Desarrollo Regional-MICINN, and Prometeo/2008/121 from the Generalitat Valenciana.

REFERENCES

Albiach-Martí, M.R., Robertson, C., Gowda, S., Tatineni, S., Belliure, B., Garnsey, S.M., Folimonova, S.Y., Moreno, P. and Dawson, W.O. (2010) The pathogenicity determinant of *Citrus tristeza virus* causing the seedling yellows syndrome maps at the 3'-terminal region of the viral genome. *Mol. Plant Pathol.* **11**, 55–67.

Bar-Joseph, M., Marcus, R. and Lee, R.F. (1989) The continuous challenge of *Citrus tristeza virus* control. *Annu. Rev. Phytopathol.* **27**, 291–316.

Baumberger, N., Tsai, C.H., Lie, M., Havecker, E. and Baulcombe, D.C. (2007) The Polerovirus silencing suppressor P0 targets ARGONAUTE proteins for degradation. *Curr. Biol.* **17**, 1609–1614.

Bortolamiol, D., Pazhouhandeh, M., Marrocco, K., Genschik, P. and Ziegler-Graff, V. (2007) The Polerovirus F box protein P0 targets ARGONAUTE1 to suppress RNA silencing. *Curr. Biol.* **17**, 1615–1621.

Bradford, M.M. (1976) A rapid and sensitive method for the quantitation of microgram quantities of protein utilizing the principle of protein–dye binding. *Anal. Biochem.* **72**, 248–254.

Carpenter, C.D. and Simon, A.E. (1998) Preparation of RNA. *Methods Mol. Biol.* **82**, 85–89.

Chiu, W., Niwa, Y., Zeng, W., Hirano, T., Kobayashi, H. and Sheen, J. (1996) Engineered GFP as a vital reporter in plants. *Curr. Biol.* **6**, 325–330.

Csorba, T., Pantaleo, V. and Burgyan, J. (2009) RNA silencing: an antiviral mechanism. *Adv. Virus Res.* **75**, 35–71.

Dellaporta, S.L., Wood, J. and Hicks, J.B. (1983) A plant DNA minipreparation: version II. *Plant Mol. Biol. Rep.* **1**, 19–21.

Díaz-Pendón, J.A. and Ding, S.W. (2008) Direct and indirect roles of viral suppressors of RNA silencing in pathogenesis. *Annu. Rev. Phytopathol.* **46**, 303–326.

Dolja, V.V., Karasev, A.V. and Koonin, E.V. (1994) Molecular-biology and evolution of closteroviruses—sophisticated buildup of large RNA genomes. *Annu. Rev. Phytopathol.* **32**, 261–285.

Dolja, V.V., Kreuze, J.F. and Valkonen, J.P. (2006) Comparative and functional genomics of closteroviruses. *Virus Res.* **117**, 38–51.

Duan, C.G., Fang, Y.Y., Zhou, B.J., Zhao, J.H., Hou, W.N., Zhu, H., Ding, S.W. and Guo, H.S. (2012) Suppression of Arabidopsis ARGONAUTE1-mediated slicing, transgene-induced RNA silencing, and DNA methylation by distinct domains of the *Cucumber mosaic virus* 2b protein. *Plant Cell*, **24**, 259–274.

Fagoaga, C., López, C., Moreno, P., Navarro, L., Flores, R. and Peña, L. (2005) Viral-like symptoms induced by the ectopic expression of the *p23* gene of *Citrus tristeza virus* are citrus specific and do not correlate with the pathogenicity of the virus strain. *Mol. Plant–Microbe Interact.* **18**, 435–445.

Fagoaga, C., Pensabene-Bellavia, G., Moreno, P., Navarro, L., Flores, R. and Peña, L. (2011) Ectopic expression of the p23 silencing suppressor of *Citrus tristeza virus* differentially modifies viral accumulation and tropism in two transgenic woody hosts. *Mol. Plant Pathol.* **12**, 898–910.

Febres, V., Ashoulin, L., Mawassi, M., Frank, A., Bar-Joseph, M., Manjunath, K., Lee, R. and Niblett, C. (1996) The p27 protein is present at one end of *Citrus tristeza virus* particles. *Phytopathology*, **86**, 1331–1335.

Folimonova, S.Y. (2012) Superinfection exclusion is an active virus-controlled function that requires a specific viral protein. *J. Virol.* **86**, 5554–5561.

Fusaro, A.F., Correa, R.L., Nakasugi, K., Jackson, C., Kawchuk, L., Vaslin, M.F. and Waterhouse, P.M. (2012) The Enamovirus P0 protein is a silencing suppressor which inhibits local and systemic RNA silencing through AGO1 degradation. *Virology*, **426**, 178–187.

Gandía, M., Conesa, A., Ancillo, G., Gadea, J., Forment, J., Pallás, V., Flores, R., Duran-Vila, N., Moreno, P. and Guerri, J. (2007) Transcriptional response of *Citrus aurantifolia* to infection by *Citrus tristeza virus*. *Virology*, **367**, 298–306.

Ghorbel, R., López, C., Fagoaga, C., Moreno, P., Navarro, L., Flores, R. and Peña, L. (2001) Transgenic citrus plants expressing the *Citrus tristeza virus* p23 protein exhibit viral-like symptoms. *Mol. Plant Pathol.* **2**, 27–36.

González, I., Martínez, L., Rakitina, D.V., Lewsey, M.G., Atencio, F.A., Llave, C., Kalinina, N.O., Carr, J.P., Palukaitis, P. and Canto, T. (2010) *Cucumber mosaic virus* 2b protein subcellular targets and interactions: their significance to RNA silencing suppressor activity. *Mol. Plant–Microbe Interact.* **23**, 294–303.

Gowda, S., Satyanarayana, T., Davis, C.L., Navas-Castillo, J., Albiach-Martí, M.R., Mawassi, M., Valkov, N., Bar-Joseph, M., Moreno, P. and Dawson, W.O. (2000) The *p20* gene product of *Citrus tristeza virus* accumulates in the amorphous inclusion bodies. *Virology*, **274**, 246–254.

Hilf, M.E., Karasev, A.V., Pappu, H.R., Gumpf, D.J., Niblett, C.L. and Garnsey, S.M. (1995) Characterization of *Citrus tristeza virus* subgenomic RNAs in infected tissue. *Virology*, **208**, 576–582.

Hsieh, Y.C., Omarov, R.T. and Scholthof, H.B. (2009) Diverse and newly recognized effects associated with short interfering RNA binding site modifications on the *Tomato bushy stunt virus* p19 silencing suppressor. *J. Virol.* **83**, 2188–2200.

Inaba, J., Kim, B.M., Shimura, H. and Masuta, C. (2011) Virus-induced necrosis is a consequence of direct protein–protein interaction between a viral RNA-silencing suppressor and a host catalase. *Plant Physiol.* **156**, 2026–2036.

Jay, F., Wang, Y., Yu, A., Taconnat, L., Pelletier, S., Colot, V., Renou, J.P. and Voinnet, O. (2011) Misregulation of *AUXIN RESPONSE FACTOR 8* underlies the developmental abnormalities caused by three distinct viral silencing suppressors in Arabidopsis. *PLoS Pathog.* **7**, e1002035.

Jensen, W.A. (1962) *Botanical Histochemistry: Principles and Practice*. San Francisco, CA: W.H. Freeman.

Kanazawa, A., Inaba, J., Shimura, H., Otagaki, S., Tsukahara, S., Matsuzawa, A., Kim, B.M., Goto, K. and Masuta, C. (2011) Virus-mediated efficient induction of epigenetic modifications of endogenous genes with phenotypic changes in plants. *Plant J.* **65**, 156–168.

Karasev, A.V., Boyko, V.P., Gowda, S., Nikolaeva, O.V., Hilf, M.E., Koonin, E.V., Niblett, C.L., Cline, K., Gumpf, D.J. and Lee, R.F. (1995) Complete sequence of the *Citrus tristeza virus* RNA genome. *Virology*, **208**, 511–520.

Lewsey, M., Robertson, F.C., Canto, T., Palukaitis, P. and Carr, J.P. (2007) Selective targeting of miRNA-regulated plant development by a viral counter-silencing protein. *Plant J.* **50**, 240–252.

López, C., Ayllón, M.A., Navas-Castillo, J., Guerri, J., Moreno, P. and Flores, R. (1998) Molecular variability of the 5'- and 3'-terminal regions of citrus tristeza virus RNA. *Phytopathology*, **88**, 685–691.

López, C., Navas-Castillo, J., Gowda, S., Moreno, P. and Flores, R. (2000) The 23-kDa protein coded by the 3'-terminal gene of *Citrus tristeza virus* is an RNA-binding protein. *Virology*, **269**, 462–470.

Lu, R., Folimonov, A., Shintaku, M., Li, W.X., Falk, B.W., Dawson, W.O. and Ding, S.W. (2004) Three distinct suppressors of RNA silencing encoded by a 20-kb viral RNA genome. *Proc. Natl. Acad. Sci. USA*, **101**, 15 742–15 747.

Lukhovitskaya, N.I., Solovieva, A.D., Boddeti, S.K., Thaduri, S., Solovyev, A.G. and Savenkov, E.I. (2013) An RNA virus-encoded zinc-finger protein acts as a plant transcription factor and induces a regulator of cell size and proliferation in two tobacco species. *Plant Cell*, **25**, 960–973.

Medberry, S.L., Lockhart, B.E. and Olszewski, N.E. (1992) The *commelina yellow mottle virus* promoter is a strong promoter in vascular and reproductive tissues. *Plant Cell*, **4**, 185–192.

Moreno, P., Guerri, J., Ballester-Olmos, J.F., Albiach-Martí, M.R. and Martínez, M.E. (1993) Separation and interference of strains from a *Citrus tristeza virus* isolate evidenced by biological activity and double-stranded RNA (dsRNA) analysis. *Plant Pathol.* **42**, 35–41.

Moreno, P., Ambrós, S., Albiach-Martí, M.R., Guerri, J. and Peña, L. (2008) *Citrus tristeza virus*: a pathogen that changed the course of the citrus industry. *Mol. Plant Pathol.* **9**, 251–268.

Navas-Castillo, J., Albiach-Martí, M.R., Gowda, S., Hilf, M.E., Garnsey, S.M. and Dawson, W.O. (1997) Kinetics of accumulation of *Citrus tristeza virus* RNAs. *Virology*, **228**, 92–97.

Padmanabhan, M.S., Goregaoker, S.P., Golem, S., Shiferaw, H. and Culver, J.N. (2005) Interaction of the *Tobacco mosaic virus* replicase protein with the Aux/IAA protein PAP1/IAA26 is associated with disease development. *J. Virol.* **79**, 2549–2558.

Pappu, H.R., Karasev, A.V., Anderson, E.J., Pappu, S.S., Hilf, M.E., Febres, V.J., Eckloff, R.M., McCaffery, M., Boyko, V. and Gowda, S. (1994) Nucleotide sequence and organization of eight 3' open reading frames of the Citrus tristeza closterovirus genome. *Virology*, **199**, 35–46.

Pappu, S.S., Febres, V.J., Pappu, H.R., Lee, R.F. and Niblett, C.L. (1997) Characterization of the 3' proximal gene of the Citrus tristeza closterovirus genome. *Virus Res.* **47**, 51–57.

Peña, L. and Navarro, L. (1999) Transgenic citrus. In: *Biotechnology in Agriculture and Forestry, Vol. 44, Transgenic Trees* (Bajaj, Y.P.S., ed.), pp. 39–54. Berlin/Heidelberg: Springer-Verlag.

Pfaffl, M.W. (2001) A new mathematical model for relative quantification in real-time RT-PCR. *Nucleic Acids Res.* **29**, e45.

Román, M.P., Cambra, M., Juárez, J., Moreno, P., Duran-Vila, N., Tanaka, F.A.O., Alves, E., Kitajima, E.W., Yamamoto, P.T., Bassanezi, R.B., Teixeira, D.C., Jesus Junior, W.C., Ayres, A.J., Gimenes-Fernandes, N., Rabenstein, F., Girotto, L.F. and Bové, J.M. (2004) Sudden death of citrus in Brazil: a graft-transmissible bud union disease. *Plant Dis.* **88**, 453–467.

Ruiz-Ruiz, S., Navarro, B., Gisel, A., Peña, L., Navarro, L., Moreno, P., Di Serio, F. and Flores, R. (2011) *Citrus tristeza virus* infection induces the accumulation of viral small RNAs (21–24-nt) mapping preferentially at the 3'-terminal region of the genomic RNA and affects the host small RNA profile. *Plant Mol. Biol.* **75**, 607–619.

Ruiz-Ruiz, S., Soler, N., Sánchez-Navarro, J., Fagoaga, C., López, C., Navarro, L., Moreno, P., Peña, L. and Flores, R. (2013) *Citrus tristeza virus* p23: determinants for nucleolar localization and their influence on suppression of RNA silencing and pathogenesis. *Mol. Plant–Microbe Interact.* **26**, 306–318.

Sambade, A., López, C., Rubio, L., Flores, R., Guerri, J. and Moreno, P. (2003) Polymorphism of a specific region in gene *p23* of *Citrus tristeza virus* allows discrimination between mild and severe isolates. *Arch. Virol.* **148**, 2325–2340.

Satyanarayana, T., Gowda, S., Boyko, V.P., Albiach-Martí, M.R., Mawassi, M., Navas-Castillo, J., Karasev, A.V., Dolja, V., Hilf, M.E., Lewandowski, D.J., Moreno, P., Bar-Joseph, M., Garnsey, S.M. and Dawson, W.O. (1999) An engineered closterovirus RNA replicon and analysis of heterologous terminal sequences for replication. *Proc. Natl. Acad. Sci. USA*, **96**, 7433–7438.

Satyanarayana, T., Gowda, S., Mawassi, M., Albiach-Martí, M.R., Ayllon, M.A., Robertson, C., Garnsey, S.M. and Dawson, W.O. (2000) Closterovirus encoded HSP70 homolog and p61 in addition to both coat proteins function in efficient virion assembly. *Virology*, **278**, 253–265.

Satyanarayana, T., Gowda, S., Ayllon, M.A., Albiach-Martí, M.R., Rabindran, S. and Dawson, W.O. (2002) The p23 protein of *Citrus tristeza virus* controls asymmetrical RNA accumulation. *J. Virol.* **76**, 473–483.

Satyanarayana, T., Gowda, S., Ayllon, M.A. and Dawson, W.O. (2004) Closterovirus bipolar virion: evidence for initiation of assembly by minor coat protein and its restriction to the genomic RNA 5' region. *Proc. Natl. Acad. Sci. USA*, **101**, 799–804.

Schneider, H. (1959) The anatomy of tristeza-virus-infected citrus. In: *Citrus Virus Diseases* (Wallace, J.M., ed.), pp. 73–84. Berkeley, CA: University of California, Division of Agricultural Sciences.

Soler, N., Plomer, M., Fagoaga, C., Moreno, P., Navarro, L., Flores, R. and Peña, L. (2012) Transformation of Mexican lime with an intron-hairpin construct expressing untranslatable versions of the genes coding for the three silencing suppressors of *Citrus tristeza virus* confers complete resistance to the virus. *Plant Biotechnol. J.* **10**, 597–608.

Tatineni, S., Robertson, C.J., Garnsey, S.M., Bar-Joseph, M., Gowda, S. and Dawson, W.O. (2008) Three genes of *Citrus tristeza virus* are dispensable for infection and movement throughout some varieties of citrus trees. *Virology*, **376**, 297–307.

Tatineni, S., Robertson, C.J., Garnsey, S.M. and Dawson, W.O. (2011) A plant virus evolved by acquiring multiple nonconserved genes to extend its host range. *Proc. Natl. Acad. Sci. USA*, **108**, 17 366–17 371.

Voinnet, O., Pinto, Y.M. and Baulcombe, D.C. (1999) Suppression of gene silencing: a general strategy used by diverse DNA and RNA viruses of plants. *Proc. Natl. Acad. Sci. USA*, **96**, 14 147–14 152.

Yambao, M.L., Yagihashi, H., Sekiguchi, H., Sekiguchi, T., Sasaki, T., Sato, M., Atsumi, G., Tacahashi, Y., Nakahara, K.S. and Uyeda, I. (2008) Point mutations in helper component protease of *Clover yellow vein virus* are associated with the attenuation of RNA-silencing suppression activity and symptom expression in broad bean. *Arch. Virol.* **153**, 105–115.

Zhang, X., Yuan, Y.R., Pei, Y., Lin, S.S., Tuschl, T., Patel, D.J. and Chua, N.H. (2006) *Cucumber mosaic virus*-encoded 2b suppressor inhibits Arabidopsis Argonaute1 cleavage activity to counter plant defense. *Genes Dev.* **20**, 3255–3268.

Ziebell, H. and Carr, J.P. (2009) Effects of dicer-like endoribonucleases 2 and 4 on infection of *Arabidopsis thaliana* by *Cucumber mosaic virus* and a mutant virus lacking the 2b counter-defence protein gene. *J. Gen. Virol.* **90**, 2288–2292.